CrossMark

Trend and recovery of the total ozone column in South America and Antarctica

Richard Toro A.[1] · Consuelo Araya[1] · Felipe Labra O.[2] · Luis Morales[2] ·
Raúl G. E. Morales[1] · Manuel A. Leiva G.[1]

Abstract South America is one of the most vulnerable areas to stratospheric ozone depletion; consequently, an increased amount of UV radiation reaches the Earth's surface in this region. In this study, we analyzed the long-term trend in the total ozone column (TOC) over the southern part of the South American continent from 1980 to 2009. The database used was obtained by combining several satellite measurements of the TOC on a 1° (latitude) × 1.25° (longitude) grid. Analysis of the long-term trend was performed by applying the Theil-Sen estimator and the Mann–Kendall significance test to the deseasonalized time series. The long-term trend was also analyzed over several highly populated urban zones in the study area. Finally, multiple linear regression (MLR) modeling was used to identify and quantify the drivers of interannual variability in the TOC over the study area with a pixel-by-pixel approach. The results showed a decrease in the TOC ranging from −0.3 to −4% dec^{-1} from 1980 to 2009. On a decadal timescale, there is significant variability in this trend, and a decrease of more than −10% dec^{-1} was found at high latitudes (1980–1989). However, the trends obtained over much of the study area were not statistically significant. Considering the period from 1980 to 1995, we found a decrease in the TOC of −2.0±0.6% dec^{-1} at latitudes below 40° S and −6.9±2.0% dec^{-1} at latitudes above 40° S, for a 99.9% confidence level over most of the study area. Analysis of the period from 1996 to 2009 showed a statistically significant increase of 2.3±0.1% dec^{-1} at high latitudes (> 60° S), confirming the initial TOC recovery in the Antarctic. Despite evidence for initial recovery of the TOC in some parts of the study area between 1996 and 2009, the long-term increase from September to November is not yet statistically significant. In addition, large parts of the study area and most of the urban areas continue to show a decreasing trend in the TOC. The MLR results show that at high latitudes, the main driver of interannual variability in the TOC is the total effective amount of halogens, followed by the eddy heat flux.

1 Introduction

Ozone (O_3) only represents 0.0012% of the total composition of the atmosphere (Iqbal 1983). Nearly 90% of atmospheric ozone is present in the stratosphere, which is located at altitudes ranging from 10 to 50 km (WMO 2010). Thus, we refer to the region of the atmosphere with the greatest proportion of ozone as the ozone layer. The ozone (O_3) layer shields Earth's living organisms from harmful ultraviolet solar radiation (UV).

The presence of the ozone layer was first determined in the 1920s based on observations of the UV solar spectrum (Lindfors and Vuilleumier 2005; Staehelin et al. 1994, 1998, 2009). The oldest and most systematic ozone column measurements were performed in Arosa, Switzerland (46°47′N, 09°41′E) beginning in 1926 (Rieder et al. 2010a, b; Staehelin et al. 1998). In 1930, the British scientist

✉ Manuel A. Leiva G.
manleiva@uchile.cl; manleiva@me.com

[1] Department of Chemistry and Center for Environmental Sciences, Faculty of Science, University of Chile, Las Palmeras 3425, PO 7800003, Ñuñoa, Santiago, Chile

[2] Faculty of Agricultural Sciences, University of Chile, Av. Santa Rosa, 11315, PO 8820808, La Pintana, Santiago, Chile

Sydney Chapman laid the foundation for current understanding of the mechanisms of ozone formation (Chapman 1930). Chapman proposed that oxygen photolysis is responsible for ozone formation and destruction. However, later studies showed that the Chapman cycle overestimated ozone concentrations. In the 1950s and the following three decades, catalytic reactions were demonstrated to participate in the destruction of ozone (Bates and Nicolet 1950; Nicolet 1955). Measurements in the Antarctic began in 1956 at the Halley Bay Observatory (76°S, 27°W) operated by the British Antarctic Survey (BAS 2012; Fogg 2000). These and other measurements provided evidence for a drastic decrease in the total ozone column (TOC) concentration towards the end of the 1970s (Godin-Beekmann 2010; Harris et al. 2008; Sola and Lorente 2010; Staehelin et al. 1998, 2001). In 1974, chlorofluorocarbons were identified as the major source of stratospheric chlorine compounds (Molina and Rowland 1974). However, it was not until the mid-1980s that these results were confirmed through satellite measurements, which showed that TOC losses of over 220 DU (Dobson units; 1 DU $= 2.69 \times 10^{16}$ molecules/cm²) occurred during spring and summer over the Antarctic, giving rise to what became known as the hole in the ozone layer.

These studies clearly showed that the ozone layer was being affected by human activities. In 1981, the Governing Council of the United Nations Environment Program (UNEP) established a working group to prepare a global framework convention for the protection of the ozone layer (Kaniaru 2007). The objective was to draft a treaty to address the depletion of the ozone layer (UNEP 2003). In 1987, the Montreal Protocol on Substances that Deplete the Ozone Layer was adopted; the protocol mandated phasing out the production and use of ozone depleting substances. These chemicals were commonly used in refrigeration, air-conditioning, foam manufacturing, aerosol production, and fire extinguishing. Current understanding indicates that reductions in the TOC follow seasonal patterns due to the dynamic coupling of heterogeneous chemical processes, meteorological processes and other phenomena that transcend quasi-periodic and non-periodic occurrences and that these reductions are affected by human activities (Antón et al. 2011; Austin et al. 2010; Harris et al. 2008; Jiang et al. 2008a, b; Kane et al. 1998a).

Because of its proximity to the depleted part of the ozone layer, South America is one of the area's most vulnerable to the increase in UV radiation at the Earth's surface that results from these reductions in the TOC. The ozone hole has directly affected South America since the 1990s. Ozone levels have decreased to 70% in certain regions (de Laat et al. 2010; Malanca 2005; Perez-Albinana et al. 2000; Weatherhead et al. 2000). For example, studies performed in the city of Punta Arenas (53°10′S, 70°56′W),

located at the southern tip of Chile, have shown that the ozone hole has expanded over the city on 44 occasions during the 1990s, including 1997, 1998 and 2000; some episodes lasted three to four days (Casiccia et al. 2003; Casiccia and Zamorano 2008; Kane 1998b; Kanitz et al. 2011; Kirchhoff et al. 1997; Monreal McMahon et al. 2002). During these episodes, measurements indicated that UVB radiation increased by nearly 80% compared to normal conditions (WMO 2010).

The hole in the ozone layer over the Southern Hemisphere reached a historical maximum on September 24, 2006; it covered 29.6 million km² and had a minimum ozone concentration of 84 DU (NASA 2012). On September 16, 2013, the hole covered a maximum area of 24 million km² and had a minimum ozone concentration of 116 DU. The Assessment for Decision-Makers is a summary document from the Scientific Assessment of Ozone Depletion: 2014, produced by the UNEP and the World Meteorological Organization (WMO). The document includes assessments by 300 scientists and is the first of the comprehensive updates published every 4 years to conclude that the TOC is in recovery and should reach the 1980 benchmark level (the time prior to significant ozone depletion) before the middle of the century. The study of temporal and spatial variability in the TOC over different regions has become a major research area (WMO 2014).

Current understanding suggests that variability in the TOC follows seasonal patterns due to the coupling of meteorological and chemical processes in the atmosphere (Anton et al. 2011a; Austin et al. 2010; Harris et al. 2008; Jiang et al. 2008a, b; Kane et al. 1998a, b). The TOC behavior is related to phenomena such as the Quasi-Biennial Oscillation (QBO) (de Artigas and de Campra 2010), the 11-year solar cycle (YSC) (Labitzke and VanLoon 1997; Ningombam 2011), the El Niño-Southern Oscillation (ENSO) (Ziemke and Chandra 2003; Ziemke et al. 2010), volcanic aerosols (AERO, the stratospheric aerosol optical thickness at 550 nm) (Geller and Smyshlyaev 2002; Lee and Smith 2003), the Artic and Antarctic Oscillations (AO and AAO) (Albinana et al. 2000; Hassler et al. 2011), ozone-depleting substances containing chlorine (EESC, equivalent effective stratospheric chlorine) (Anton et al. 2011b), and the winter accumulated eddy heat flux at 100 mb (EHF) (Weber et al. 2011; Chehade et al. 2014). In general, the effect of these factors on TOC variability has been studied using numerical models and linear approximations (e.g., Anton et al. 2010; Jain et al. 2008; Tandon and Attri 2011).

The goal of this study was to examine variations in the TOC at various time scales (monthly, seasonal and yearly) and identify the trends at these timescales over three decades (1980–2009) in the southern part of South America (the geographic area between 0°–90°S and 33°–107°W).

For this purpose, we obtained data from several satellite-based sources, and also used a merged TOC database that has already been validated and used in several studies (Cionni et al. 2011; Harris et al. 2003; Müller et al. 2008; Struthers et al. 2009). We aim to enhance the present state of knowledge and to provide a better evaluation of spatial and temporal trends in the TOC over South America.

2 Experimental section

2.1 Description of the database

Satellite measurements of the total ozone concentration in the atmosphere have been crucial for studying spatial and temporal variations in the TOC on both a global and regional scale (Krueger et al. 1980). Several satellites have obtained high quality time series of ozone in the atmosphere using various operational remote sensors, including the Total Ozone Mapping Spectrometer (TOMS, http://ozoneaq.gsfc.nasa.gov), the Ozone Monitoring Instrument (OMI, http://knmi.nl/omi/), the Global Ozone Monitoring Experiment (GOME, http://earth.esa.int/eeo4.96) and the Solar Backscatter Ultraviolet Radiometer-2 (SBUV/2, http://orbit.nesdis.noaa.gov/smcd/spb/ozone/). The data used in this study were obtained from the Bodeker Scientific 2.8 database, version 2.8, of the global and daily patched total column ozone from 1980 to 2009. The database was produced by combining the ozone measurements over a 1° (latitude) × 1.25° (longitude) grid of data compiled from various satellite measurements. The merged satellite data include TOMS version 8, TOC retrievals based on using the TOMS version 8 retrieval algorithm for OMI data, GOME version 4.0 ozone retrievals, the GOME TOC fields from the Royal Netherlands Meteorological Institute's (KNMI's) TOGOMI algorithm and Solar Backscatter Ultra-Violet (SBUV) version 8. Descriptions of the datasets are available in a number of publications (Bodeker et al. 2005; Müller et al. 2008; Struthers et al. 2009). The database is available in netCDF format from Bodeker Scientific (http://www.bodekerscientific.com).

2.2 Database analysis

IDRISI® Selva software version 17 for Windows® (Clark Labs at Clark University, Worcester, MA) was used to analyze TOC concentrations over South America. First, we imported the database in netCDF format and obtained a raster image format (*.rst). Second, the rst-formatted images were cropped to the area of interest. The study area was 0°–90° S and 33°–107° W. Finally, the cropped rst-formatted images were grouped into 10-year periods to obtain groups of raster images (*.rgf) for 1980–1989, 1990–1999

and 2000–2009 and for the total study period from 1980 to 2009. Following these database operations, we analyzed the spatial and temporal variability over the study area.

2.3 Long-term trend analysis

The long-term trend over the study area was evaluated for all three 10-year periods and the 30-year period (1980–1989, 1990–1999, 2000–2009 and 1980–2009). Analysis was performed using the ETM module, specifically the Theil-Sen (TS) estimator and non-parametric Mann–Kendall (MK) statistical tests. These statistical tests are widely used to analyze trends in air pollutants (Munir et al. 2013; Toro et al. 2014).

Two-tailed Z-score results from the MK significance test were used to determine whether the trend was statistically significant. A positive Z-score indicates an increasing trend and a negative value indicates a decreasing trend. We accepted or rejected the null hypothesis (H_0) that there was no trend depending on whether the computed absolute value of the Z-scores ($|Z\text{-}scores|$) was greater than the critical value of the Z-score statistics ($|Z-scores|^{p-value}_{critical}$) at the determined significance ($p\text{-}value$). We analyzed the results of the MK significance test for two p-values: 0.950 ($|Z-scores|^{0.950}_{critical} = 1.96$) and 0.999 ($|Z-scores|^{0.999}_{critical} = 3.29$). The TS test is related to the magnitude of the trend ($slope$) found by the MK test. The slope (in DU month^{-1}) was used to calculate the magnitude of variations in the TOC in % change per decade (%dec^{-1}). The deseason option was used.

We also analyzed the long-term trend over several densely populated urban areas located in the study area: Sao Paulo, Montevideo, Rio de Janeiro, Buenos Aires, Belo Horizonte, Asunción, Brasilia, Santiago, Salvador, Lima and La Paz. In addition, two cities in Patagonia (Punta Arenas, Chile and Ushuaia, Argentina) were analyzed due to their proximity to the Antarctic ozone hole, and one pixel in the Antarctic was selected. The Openair software package was used for analysis (Carslaw and Ropkins 2012). As with the continental-scale analyses, the analysis of temporal trends for each city was estimated using the TS and MK approach and the deseason option.

2.4 Multivariate linear regression model

Trends in global total ozone were investigated using a multivariate linear regression (MLR) model. The model included various explanatory parameters (as discussed above) that account for chemical and dynamic processes in the atmosphere (WMO 2010, 2014). The annual mean total ozone column (TOC) time series was constructed based on a simple linear sum of explanatory variables, or driving factors, as follows:

$$\begin{aligned}
\text{TOC}(t) = {}& \text{TOC}(t) + \gamma^{\text{YSC}}\text{YSC}(t) + \gamma^{\text{ENSO}}\text{ENSO}_{1+2}(t) \\
& + \gamma^{\text{QBO10}}\text{QBO}_{10}(t) + \gamma^{\text{QBO30}}\text{QBO}_{30}(t) \\
& + \gamma^{\text{AAO}}\text{AAO}(t) + \gamma^{\text{EESC}}\text{EESC}(t) + \gamma^{\text{EHF}}\text{EHF}(t) \\
& + \gamma^{\text{AERO}}\text{AERO}(t) + \text{RES}(t)
\end{aligned} \quad (1)$$

where t is a running index (from zero to 29) corresponding to all years from 1980 to 2009, γ^{X} is the time dependent regression coefficient of each proxy (X) and RES(t) is the residual error of the series for the regression model, which includes sporadic events and other parameters that are not considered. The proxies are 11-year solar cycle (YSC), Niño Southern Oscillation (ENSO), The quasi-biennial oscillation (QBO), Antarctic Oscillation (AAO), atmospheric volcanic aerosols (AERO), equivalent effective stratospheric chlorine (EESC) and eddy heat flux (EHF). Below is a brief description for each proxy.

YSC was used as a proxy to investigate the impact of UV solar irradiance modulation. YSC is considered a dominant form of long-term ozone changes and has been included in all ozone trend assessments (WMO 2010, 2014). Previous studies found that at mid-latitudes about 2% of total ozone variability can be explained through changes in the solar cycle (Shindell et al. 1999). YSC it is included as solar flux measured at a wavelength of 10.7 cm. The 10.7 cm solar flux data were obtained from the National Research Council of Canada (http://www.spaceweather.ca/solarflux/sx-4-eng.php).

ENSO proxy is linked with the cycling of a Pacific Ocean circulation pattern (Horel and Wallace 1981; Karoly 1989). Various studies have shown that the ENSO signal affects the dynamics of the lower stratosphere, including the amount of ozone (Randel et al. 2002; Ziemke et al. 2010). During El Nino (Niña) events, a positive (negative) values of index, an increase (decrease) in dynamical convection from ENSO events in the tropical Pacific induces a decrease (increase) in tropospheric column ozone (Shiotani 1992). For ENSO, the Niño $1+2$ region (ENSO_{1+2}, 0°–10°S, 80°W–90°W) is included in the regression. ENSO index data were obtained from the Climate Prediction Center (CPC) of the National Oceanic and Atmospheric Administration (NOAA) (http://www.esrl.noaa.gov/psd/data/climateindices/list/).

QBO is a quasiperiodic oscillation of the equatorial zonal wind between easterlies and westerlies in the tropical stratosphere with a mean period of 28–29 months. The effect of the quasi-biennial oscillation (QBO) in easterly and westerly stratospheric winds in the tropics on stratospheric ozone is a well-established (McCormack et al. 2007; Witte et al. 2008; WMO 2010). In this study, the QBO at two different pressure levels (10 and 30 hPa) was used (from FU Berlin, http://www.geo.fuberlin.de/

en/met/ag/strat/produkte/qbo/index.html) in the regression analysis.

The Antarctic Oscillation (AAO) was defined as a belt of westerly winds or low pressure surrounding Antarctica, with its mode of variability described by its movement to the north or south. AAO. Studies have shown that AAO affects ozone concentration by limiting circulation from the tropics to the polar region, in the high phases, or vice versa in the low phases (Frossard et al. 2013). The AAO index was obtained from NOAA's National Weather Service CPC (http://www.cpc.ncep.noaa.gov/products/precip/CWlink/daily_ao_index/teleconnections.shtml).

Perturbations in atmospheric volcanic aerosols (AERO) affect stratospheric ozone directly via changes in heterogeneous chemistry and photolysis rates and indirectly via changes in stratospheric temperature and large-scale circulation patterns (SPARC 2006). In order to take account the AERO we used the time dependent stratospheric aerosol optical depth (OD) at 550 nm (Sato et al. 1993).

The scale of EESC (equivalent effective stratospheric chlorine) describes the effect of stratospheric ozone depletion caused by anthropogenic emissions of ozone depleting substances, such as chlorofluorocarbons. EESC parameter is used to quantify man-made ozone depletion and its changes with time. These parameter was included in the model to account for the chemical processes of ozone depletion (http://acdb-ext.gsfc.nasa.gov/Data_services/automailer/index.html).

Finally, EHF describe the movement of the wave system and temperature variation by the weather systems in the troposphere. The upward propagation of weather systems warms the polar region. Strong positive fluxes indicate poleward flux of heat via eddies. We use the 100 hPa EHF averaged over mid-latitudes between 45°S and 75°S as a proxy for ozone transport due to variation in planetary wave driving. EHF was obtained from CPC of NOA.

For all proxies, the annual mean data obtained by averaging monthly mean values are used with no time lags. Only for AAO, a winter mean (Jun-Jul-Aug for the Southern Hemisphere) was used. This process resulted in global fields that describe the geographical distribution of each explanatory variable.

The MLR results are expressed in terms of adjusted correlation coefficients (adjusted-R^2), standardized partial correlation coefficients (Partial-R) and twice the standard deviation (2σ) of the variability attributable to each proxy. The adjusted-R^2 varies between 0 and 1; a value of 1 indicates that the model explains 100% of the interannual variability of the TOC, and a value of 0 indicates that the model can explain none of the variability. Adjusted-R^2 values larger than approximately 0.6 indicate that the regression describes a large part of the variability (more than 60%). The partial-R of correlation indicates the strength

of association between a dependent variable and an independent variable when the effect of all other independent variables is removed. The partial-R can range in values from −1 to +1; a positive partial correlation implies that as the values of one variable increase, so do the values of a second variable (while the values of the other proxies are held constant). The standardized partial correlation coefficients were obtained one variable at a time. The 2σ variable is defined from the corresponding time series term on the right side of Eq. (1). The value of this term is based on the average minimum-to-maximum variation attributed to an explanatory variable X. Brown to yellow colors indicate a positive correlation (partial-R > 0) and magenta to green colors indicate a negative correlation (partial-R < 0). Thus, the sign indicates a positive or negative fluctuation and the size indicates the magnitude of fluctuation attributable to a given ozone proxy in the MLR. Using 2σ allows comparison of the importance of different explanatory variables to explain the interannual variability of TOC.

The time series of explanatory variables used in MLR analysis must be fully independent (uncorrelated). In this study, the correlations between the predictors are very small (reaching a maximum of 0.29). We also used the Durbin-Watson (DW) statistic to detect first order autocorrelations present in the residuals of the regression analysis (Durbin and Watson 1950). DW values should always be between 0 and 4; a value of 2 indicates no autocorrelation in the data, and values from 1 to 3 are assumed to indicate insignificant autocorrelation. For our MLR model, we found DW values between 1.30 and 2.45 (except some pixels on Los Andes Mountains with DW values < 1.30), confirming the reliability of the model.

3 Results and discussion

3.1 Descriptive analysis

The top panel in Fig. 1 shows the average of the TOC in the study area for 1980–1989 (Fig. 1, a1), 1990–1999 (Fig. 1, a2), 2000–2009 (Fig. 1, a3) and 1980–2009 (Fig. 1, a4). The time series of area-weighted monthly TOC concentrations are shown in Fig. 1b, along with their respective area-weighted standard deviations for the 30 years of the study period. These are shown for low (0°–30°S, Fig. 1, b1), middle (30°–60° S, Fig. 1, b2) and high latitudes (60°–90° S, Fig. 1, b3). Figure 1c shows the intra-annual variability of the average TOC for each month of the study period.

Figure 1a shows that the TOC values ranged from 240 DU to 310 DU in the study area. During all four time periods considered, a latitudinal layering of the TOC was observed. The highest TOC values (≈300 DU) were found at mid-latitudes (30°–60° S, yellow and red colors in Fig. 1a), and the lowest TOC values were observed at high latitudes (60°–90° S, cyan and magenta colors) and over the Andes Mountains (approximately 0°–30° S and 60°–80° W). Transition areas in the TOC were also apparent (≈275 DU, Fig. 1a) at middle-low (30°S) and middle-high (60°S) latitudes. This latitudinal TOC variability has been previously documented (Niu et al. 1992; Kane et al. 1998a; Malanca 2005; Werner 2008; Austin et al. 2010); it is caused by transport phenomena and the redistribution of stratospheric ozone due to the Brewer–Dobson circulation (BDC) and photochemical depletion (Brewer 1949; Dobson 1956).

The time series of the monthly averaged TOC concentrations over the 30-year study period at low (0–30°S, Fig. 1, b1), middle (30°–60°S, Fig. 1, b2) and high latitudes (60°–90°S, Fig. 1, b3) show that the average TOC concentrations were 262 ± 9, 296 ± 19 and 263 ± 38 DU, respectively. The highest TOC concentrations were observed from 1980 to 1989, when values of 264 ± 9, 302 ± 18 and 275 ± 30 DU were reached at low, middle and high latitudes, respectively. The lowest TOC concentrations were observed from 1990 to 1999 and 2000–2009, with constant values of 261 ± 9 and 293 ± 19 DU at low and middle latitudes, respectively. However, there was a slight difference in TOC concentrations at high latitudes during these decades; they averaged 254 ± 40 and 260 ± 38 DU from 1990 to 1999 and 2000–2009, respectively. This difference could indicate a change in the ozone trend at high latitudes, which was confirmed by subsequent analysis (below). Seasonal variability is also apparent in the time series. This variability was expressed as the average amplitude for the 30-year study period (i.e., the difference between the average maximum and minimum TOC values for each year). This seasonal variability increases with latitude; the lowest amplitude occurs at low latitudes (25 ± 10 DU), followed by middle (53 ± 17 DU) and high latitudes (116 ± 44). Figure 1c shows the intra-annual TOC variability at low, middle and high latitudes. The TOC increases during the winter (July–September) and early spring (October) at low and middle latitudes in the Southern Hemisphere. This increase occurs because during this time of the year, ozone transport to these areas is stronger than ozone-depleting processes, which are less efficient during the winter in the Southern Hemisphere. Thus, the highest ozone concentrations are found from September to October. The maximum average values for this period were found at low (276 ± 4 DU) and middle (325 ± 10 DU) latitudes. However, there is a decrease in ozone at the end of the summer, from March to May, at which time the minimum TOC concentrations were observed at low (252 ± 4 DU) and middle (272 ± 6 DU) latitudes. This behavior can be explained because ozone transport to the TOC is minimized at this time; additionally,
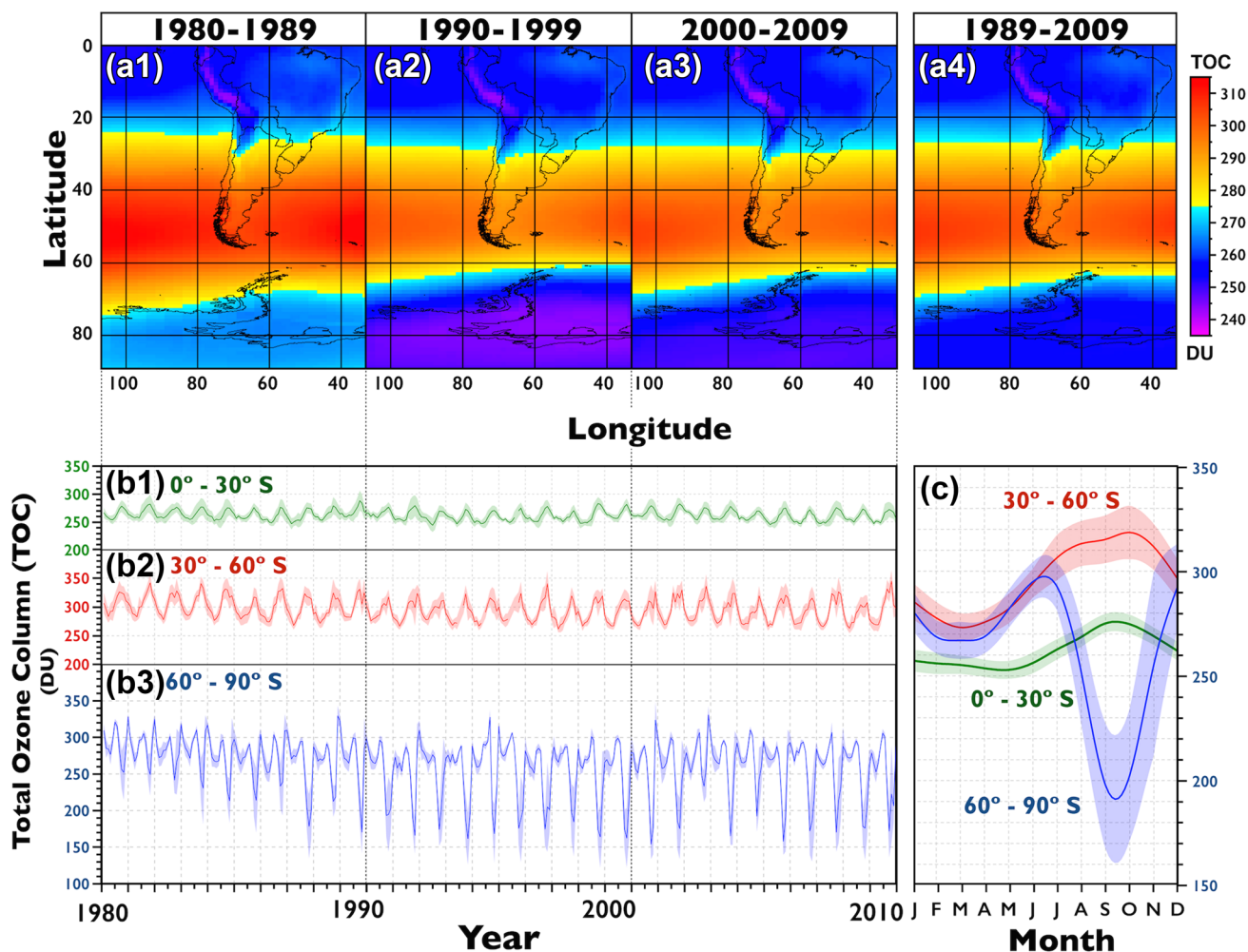
Fig. 1 Average thickness of the Total Ozone Column (TOC) in the study area from 1980 to 1989, 1990–1999, 2000–2009 and 1980–2009 (*top*) and time series of TOC over the 30-year study period (*bottom*). The time series are grouped into low (0°–30°S, *green*), middle (30°–60°S, *red*) and high latitudes (60°–90° S, *blue*). Weighted area values obtained for each month for the different groups are also (*bottom right*)

there is higher photochemical ozone depletion due to the increase in solar radiation during the summer, which causes a decrease in the TOC. We note that there is an increase in TOC concentrations during early austral autumn (April) at high and middle latitudes, though the maximum value for mid-latitudes (305 ± 14 DU) occurred in June. After reaching this maximum, there is a sudden decrease in the TOC concentration during late austral winter (July–August). The lowest TOC concentration (190 ± 30 DU) was observed in late September and early October, after which the TOC levels increased to reach a value similar to the maximum value observed during December. This variability in the TOC concentration has been reported in previous studies and is due to two processes. One process is the catalytic reactions that cause ozone depletion, which are active during the spring; the second is the formation of the so-called ozone hole because of the Antarctic polar vortex.

Another notable result is the periodic behavior of the time series at middle latitudes during September or October (Fig. 1, b2, c, in red); there is a slight decrease in the TOC concentration immediately before it reaches its maximum annual value. This decrease in the TOC is observed in 18 of the 30 years of the time series studied and has become more frequent since the 1990s. Because the figure shows the area-weighted mean between 30 and 60°S, this decrease can be explained the fact that in some years, the size of the polar vortex (and therefore, the ozone hole) grows until it reaches latitudes lower than 60°S by making the column ozone decrease slightly at middle latitudes during September or October.

3.2 The TOC's seasonal cycle

Figure 2 shows the mean and standard deviation of the TOC in the study area over 30 years. The time series are grouped into 3-month periods to allow analysis of the intra-annual variability of the TOC in the study area.

Figure 2 shows that the period from December to May (i.e., summer and autumn) was characterized by mean values from 250 to 280 DU. During these seasons, large-scale atmospheric circulation redistributes the ozone generated in the inter-tropical zone, homogenizing the TOC concentration in the study area. The standard deviation observed during this period increases with latitude, reaching approximately 20 DU over Antarctica.

The formation of the Antarctic polar vortex during austral winter disrupts these large-scale circulation processes in the Southern Hemisphere by progressively isolating air masses at middle and high latitudes. The release of the chlorine that accumulates in polar stratospheric clouds during the austral spring then minimizes the TOC over Antarctica between September and November. An increase in TOC at middle latitudes occurs during this period of low circulation, resulting the highest annual mean TOC values. During the same period (Sep–Oct–Nov), the destruction of stratospheric ozone reaches its maximum on the Antarctic continent; average TOC values are below 200 DU at latitudes >70°S, and the standard deviation in the area is greater than 50 DU.

3.3 Long-term trend

Figure 3 shows the Z-scores for the TOC concentrations in the study area from 1980 to 1989, 1990–1999, 2000–2009 and 1980–2009 obtained from the significance test (Fig. 3, above), as well as the slope (DU month^{-1}) calculated using the TS estimator and the statistically significant percent variation per decade (% dec^{-1}) for a confidence level of 95%.

Positive trends (Z-scores > 0, yellow, orange and red colors) and negative trends (Z-scores < 0, cyan, blue and magenta colors) are apparent in Fig. 3 for each of the three decades and for the 30-year period. A statistically significant decrease in the TOC was observed at confidence levels of 95 and 99.9%. The Z-score values were below −1.96 at latitudes above 40°S in the 1980s (Fig. 3, a1) and below −3.29 near 20° S in the 2000s (Fig. 3, a3). However, in the 1990s (Fig. 3, a2), no statistically significant trends were found for a confidence level of 95%, indicating that
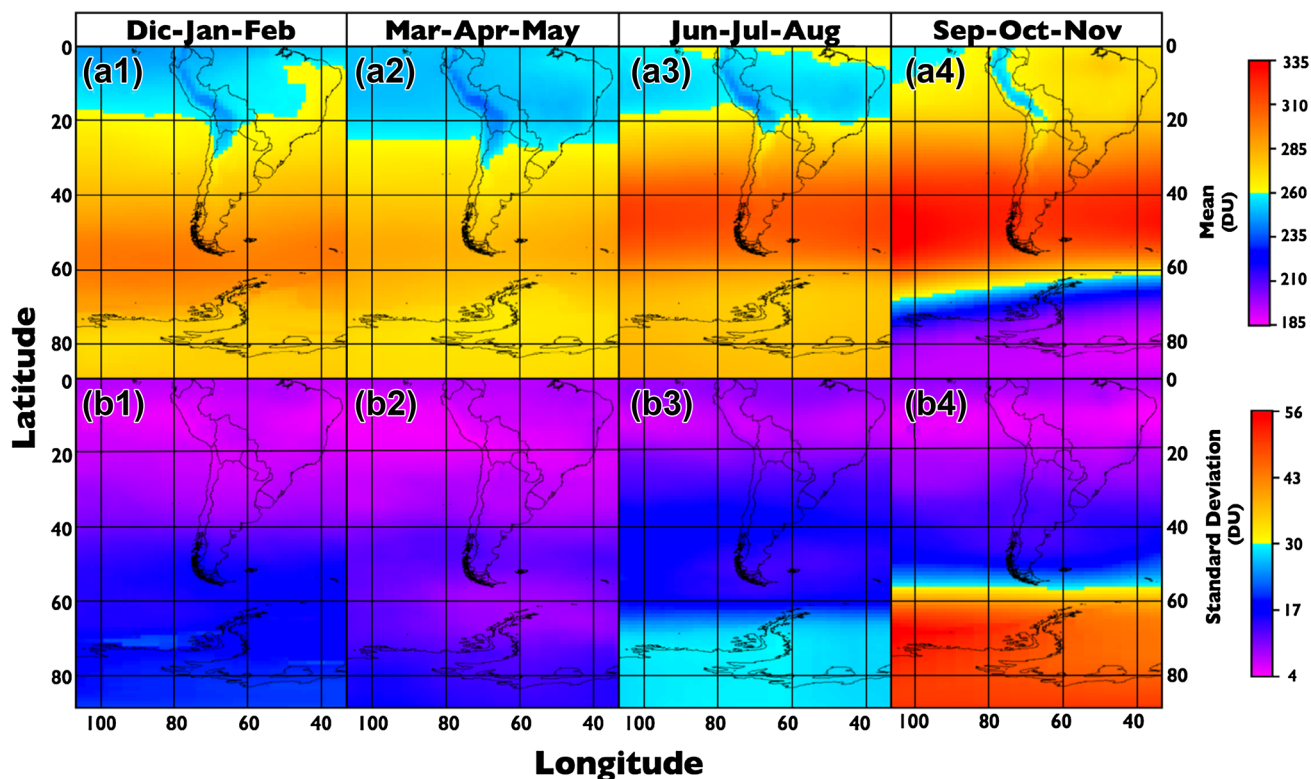

Fig. 2 Mean (*top*) and standard deviation (*bottom*) of intra-annual variations in the TOC in the study area over the 30-year study period. Data are grouped into December, January and February (Dec–Jan–Feb), March, April and May (Mar–Apr–May), June, July and August (Jun–Jul–Aug) and September, October and November (Sep–Oct–Nov)
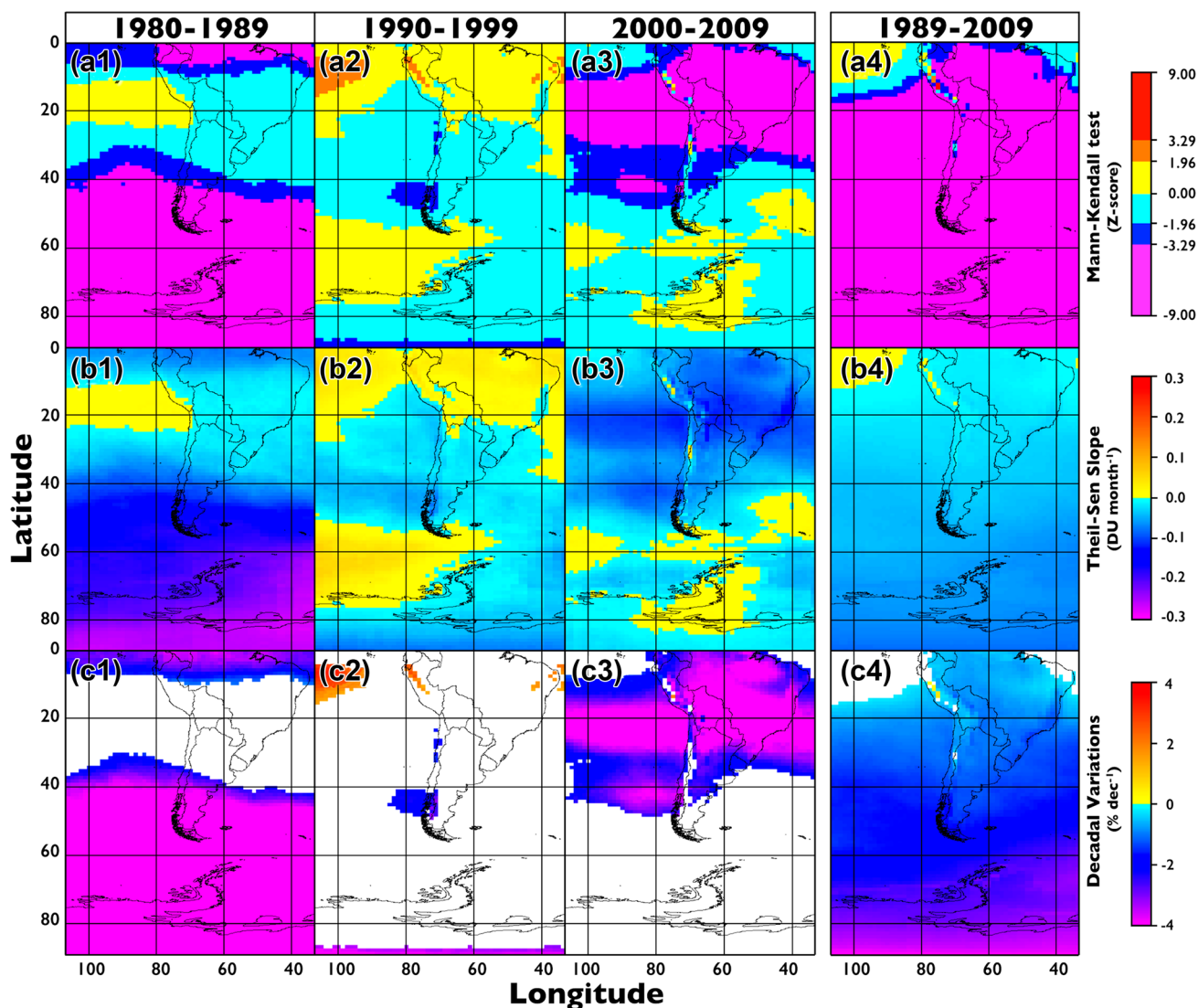
Fig. 3 Statistical significance of the trends obtained from the Mann–Kendall test expressed as Z-scores (*top*), long-term trends obtained from the slope of the Theil-Sen estimator (*middle*) and decadal variations in the TOC expressed in % dec^{-1} (*bottom*) in the study area from 1980 to 1989, 1990–1999, 2000–2009 and 1980–2009. Non-significant trends (at a 95% confidence level) are shown in *white* for Z-scores greater than 1.96 and less than −1.96 (−1.96 < Z < 1.96)

the Z-score values were between 0 and −1.96. An analysis of the trend over the entire 30-year study period reveals an increase in the statistical robustness of the estimation because the decreasing trends were significant over the majority of the study area at a confidence level of 99.9%. Statistically significant decreasing trends were found at latitudes above 20°S at a confidence level of 99.9% (Fig. 3, a4).

Increasing trends in the TOC (yellow, orange and red colors in Fig. 3, a4) can be observed during the 1980s at approximately 20° S (Fig. 3, a1). In the 2000s (Fig. 3, a3), these trends can be observed near 40° and 60°S. Positive trends are apparent during the 1990s at latitudes above 20° S and at approximately 60°S. Over the 30-year period, the

only increasing trends in the TOC were observed above 20° S (Fig. 3a). In general, these increasing trends during each of the three decades and the 30-year period were not statistically significant at a confidence level of 95%.

The magnitude of the trends obtained from the TS estimator (Fig. 3, middle panels) using the slope (DU month^{-1}) ranged from 0.1 to −0.3 DU month^{-1}. The positive and negative variability of these trends follows a similar pattern to the MK results (Fig. 3, top panels). The percent variation per decade (% dec^{-1}) was calculated based on the results of the trend magnitudes expressed in DU units (month^{-1}). These results are shown at the bottom of Fig. 3. Only the statistically significant results (at a 95% confidence level) are presented in Fig. 3; these have absolute

Z-score values greater than or equal to 1.96. The results show that decreases occurred during the 1980s and 2000s at latitudes greater than 40° S; the largest decreases in percentage occurred at latitudes over 80° S during the 1980s and at approximately 20° S during the 2000s. No statistically significant results at a 95% confidence level were observed during the 1990s. Over the entire study period (1980–2009), statistically significant decreasing trends are only observed at latitudes greater than 20° S, with values ranging from -0.3 to -4% dec^{-1}.

These results may suggest that the TOC has increased, for the following reasons: (1) non-statistically significant increasing trends (positive values) were observed at high latitudes during the 2000s; (2) the 1990s could correspond to a transition in the TOC trend from a period of decrease to a period of increase; and (3) the Theil-Sen trend estimator and the Mann–Kendall significance test only yield the slope and statistical significance of a monotonic linear regression obtained from the time series. They do not reflect the inflection points corresponding to changes between a decreasing and an increasing trend in the TOC.

Based on these results, we use a longer time series to study the statistically significant positive changes in the TOC (i.e., an increase). This approach allows us to demonstrate the initial recovery of the ozone layer over the study area with statistical certainty. Therefore, we split the time series into two periods, from 1980 to 1995 and 1996–2009.

3.4 Ozone layer recovery

Figure 4 shows the results of the Z-scores obtained from the MK significance test (Fig. 4, top), the slope (DU month^{-1}) of the TS estimator (Fig. 4, middle) and the statistically significant percent variation per decade (% dec^{-1}) at a 95% confidence level (absolute Z-score values greater than 1.96) (Fig. 4, bottom) from 1980 to 1995 and 1996–2009 over the study area.

The MK test results for 1980–1995 show a negative trend at a confidence level of 99.9% (Z-scores <-3.29, Fig. 4, a1) over nearly the entire study area. Non-significant trends $(0 > Z\text{-score} > -1.96)$ are only observed over the Andes Mountains at low latitudes. There is a notable difference between 1996 and 2009 and 1980–1995. Both positive and negative trends are apparent from 1996 to 2009 (Fig. 4, a2) at a 95% significance level ($|Z\text{-score}| > 1.96$). Statistically significant negative trends are observed at a 95% confidence level for latitudes below 40° S (blue and magenta colors in Fig. 4, a2). Positive trends are observed at latitudes above 40° S; these are statistically significant at a 95% confidence level (Fig. 4, a2) at approximately 70° S in the Antarctic region. The latter result is a clear indication of TOC recovery because it shows that statistically significant positive trends occurred at high latitudes. Regarding the

results from the TS estimator (Fig. 4b), most of the slope values ranged from -0.21 to 0.01 DU month^{-1} from 1980 to 1995 and from -0.08 to 0.06 DU month^{-1} from 1996 to 2009. The latitudinal variation is similar to the results of the MK significance test, as expected. The percent variation per decade in TOC from 1980 to 1995 showed an average decrease of $-2.0 \pm 0.6\%$ dec^{-1} at altitudes below 40°S and $-6.9 \pm 2.0\%$ dec^{-1} at latitudes above 40° S. However, from 1996 to 2009, the average TOC decreased by $-1.9 \pm 0.5\%$ dec^{-1} at approximately 20° S and increased by $2.3 \pm 0.1\%$ dec^{-1} in the Antarctic. These results are consistent with the initial stages of the recovery of the Antarctic ozone layer.

Despite the initial recovery of the Antarctic ozone layer from 1996 to 2009 (see Fig. 4c2), there were statistically significant decreasing trends in the TOC over large portions of the middle and low latitudes of the study area. These demonstrate that halogens in the stratosphere have long-term effects, and they are currently causing a decrease in the TOC at these latitudes.

3.5 Seasonal long-term trend analysis

Because of the TOC's seasonality, we estimated the decadal trends for each three-month season. Figure 5 shows the results of TOC trend analysis for each of the three-month seasons from 1980 to 1995.

There are statistically significant decreasing trends over most of the study area during all three-month seasons from 1980 to 1995. The decadal variations in Sep–Oct–Nov are greater than -8% dec^{-1}; these are the greatest long-term decreases in the TOC and the greatest intra-annual variations occur during this period (see Fig. 2). In some areas (at high latitudes during Mar-Apr-May and middle latitudes during Sep–Oct–Nov), the trends are not statistically significant. However, the TOC shows a decreasing tendency in these areas.

Figure 6 shows the results of TOC trend analysis for each three-month season from 1996 to 2009.

There are statistically significant increases in the TOC in Dec–Jan–Feb, Mar–Apr–May and Jun–Jul–Aug. These trends confirm the beginning of the TOC recovery shown in the analysis of the annual time series for 1996 to 2009 (Fig. 4).

Between December and May, this recovery is observed at high latitudes, while in Jun-Jul-Aug, the recovery is observed in the Patagonia area of Chile and Argentina, which is in the southernmost part of South America. This part of the continent is listed as a vulnerable area due to its proximity to the polar vortex, which causes significant ozone losses at middle latitudes when it breaks up during November and December because of its dilution effect. Paradoxically, the first signs of the TOC's recovery appear in

Fig. 4 Mann–Kendall test expressed as Z-scores (*top*), slope of the Theil-Sen estimator (*middle*) and decadal variations in the TOC (*bottom*) from 1980 to 1994 and 1995–2009. Non-significant trends (at a 95% confidence level) are shown in *white* ($-1.96 < Z < 1.96$)
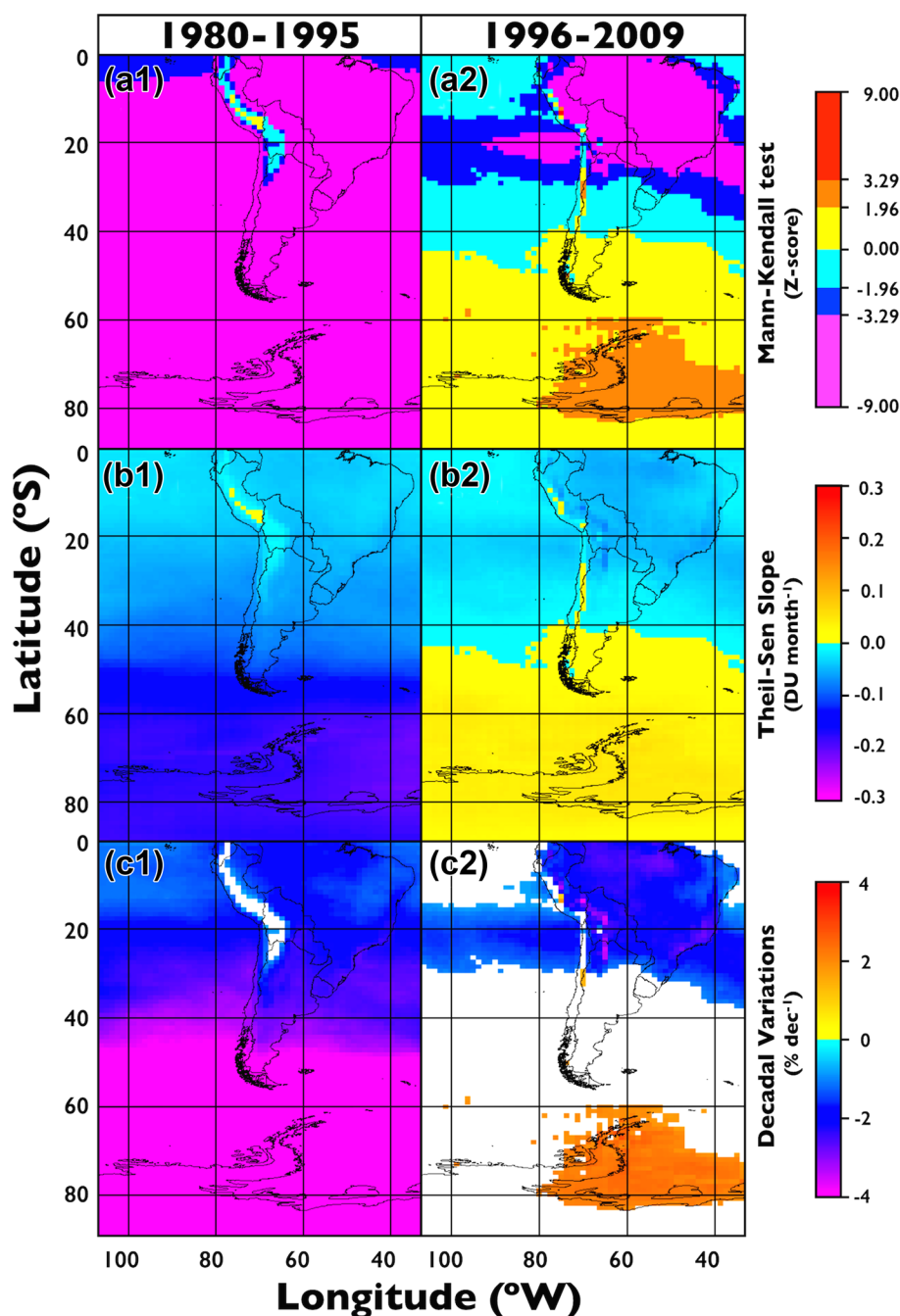
this area in both the annual results (Fig. 4) and the seasonal results (Fig. 6).

3.6 Long-term trends in the urban areas of South America

Table 1 shows temporal trends obtained using the slope of the TS estimator (% dec^{-1}) in urban areas of South America inhabited by more than 74 million people from 1980 to 1995 and 1996–2009. The 95% confidence intervals for the slope and the p-values are also presented. These values indicate the statistical significance of the trends based on the MK test.

A statistically significant decrease in the TOC ($p < 0.001$) was observed from 1980 to 1995 in all cities with the exception of La Paz ($p > 0.1$). This city is located at 3650 m.a.s.l, and no significant changes in the TOC were found during this time period. We note, however, that there was a decrease in the TOC over Quito during this period ($p < 0.01$), even though this city is located on the equator. The values of the decrease in TOC from 1980 to 1995 for the remaining cities are as follows, in descending
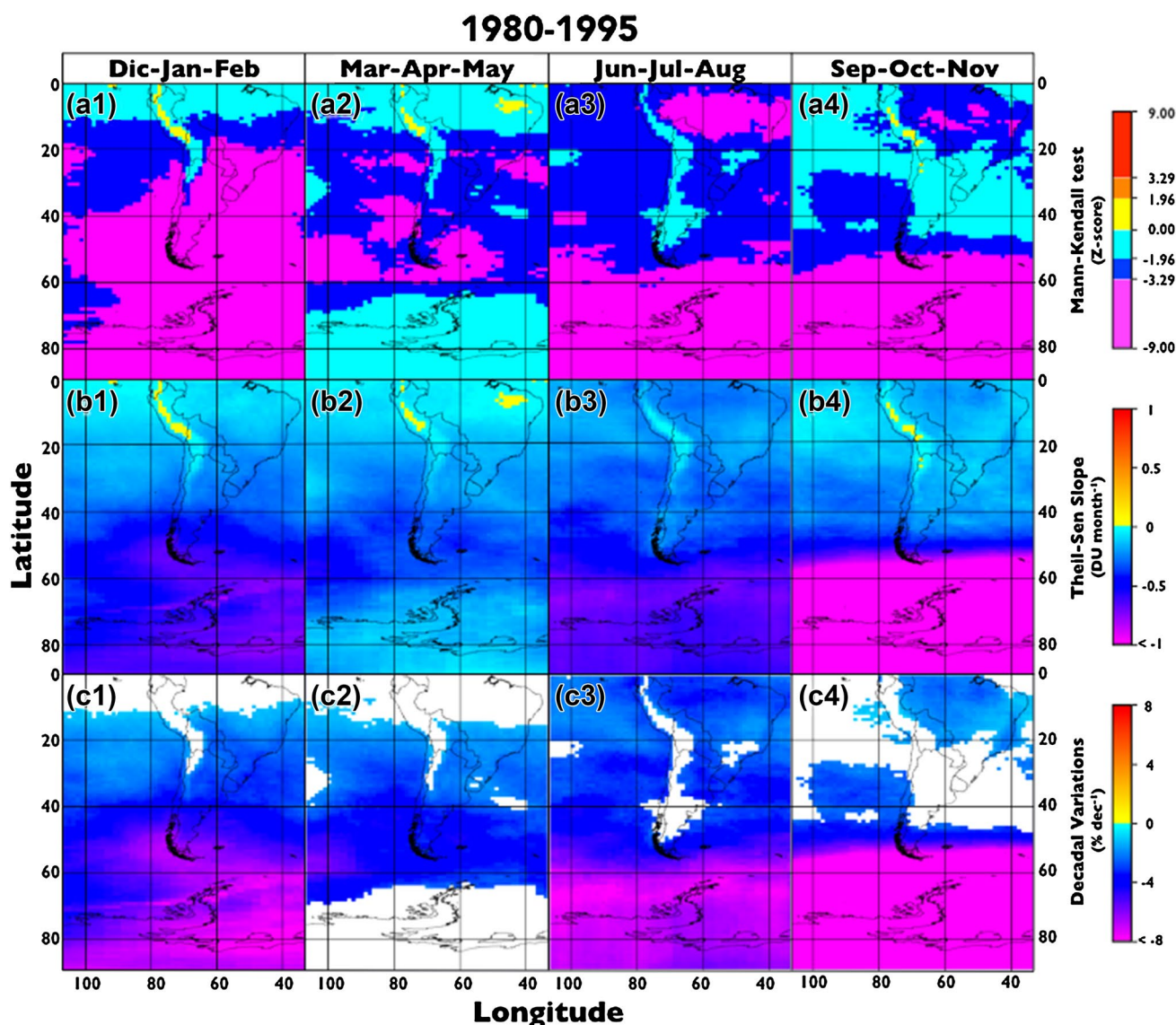
1980-1995

Fig. 5 Analysis of trends in the TOC from 1980 to 1995 for seasons defined as December, January and February (Dec–Jan–Feb), March, April and May (Mar–Apr–May), June, July and August (Jun–Jul– Aug) and September, October and November (Sep–Oct–Nov). *Plots follow the same format as in Fig. 4*

order: the Antarctic (-7.42% dec^{-1}) > Ushuaia (-5.44% dec^{-1}) > Punta Arenas (-5.09% dec^{-1}) > Sao Paulo (-2.53% dec^{-1}) ≈ Buenos Aires (-2.52% dec^{-1}) > Montevideo (-2.45% dec^{-1}) > Rio de Janeiro (-2.35% dec^{-1}) > Asunción (-2.19% dec^{-1}) > Santiago (-2.11% dec^{-1}) > Belo Horizonte (-2.05% dec^{-1}) > Salvador de Bahía (-1.86% dec^{-1}) > Guayaquil (-1.70% dec^{-1}) > Quito (-1.56% dec^{-1}) > Brasilia (-1.46% dec^{-1}) ≈ Lima (-1.46% dec^{-1}) ≈ Fortaleza (-1.44% dec^{-1}).

From 1996 to 2009, in contrast to the former period, there were increases (positive slopes) in the TOC over Ushuaia (0.97% dec^{-1}), Punta Arenas (0.61% dec^{-1}) and Santiago (0.48% dec^{-1}). However, these values were not

statistically significant (p > 0.1) because they have a slope of 0 for a 95% confidence level. Similarly, statistically significant trends (p > 0.1) were not found over Buenos Aires or Montevideo. In Quito and Guayaquil, there were statistically significant decreases at a 90% confidence level (p < 0.1); in Fortaleza and Lima, there were statistically significant decreases at a 95% confidence level (p < 0.05). In the remaining cities, there were statistically significant decreases at a 99.9% confidence level. These decreases in TOC are as follows, in descending order: Belo Horizonte (-2.40% dec^{-1}) ≈ Sao Paulo (-2.38% dec^{-1}) > Rio de Janeiro (-2.15% dec^{-1}) ≈ La Paz
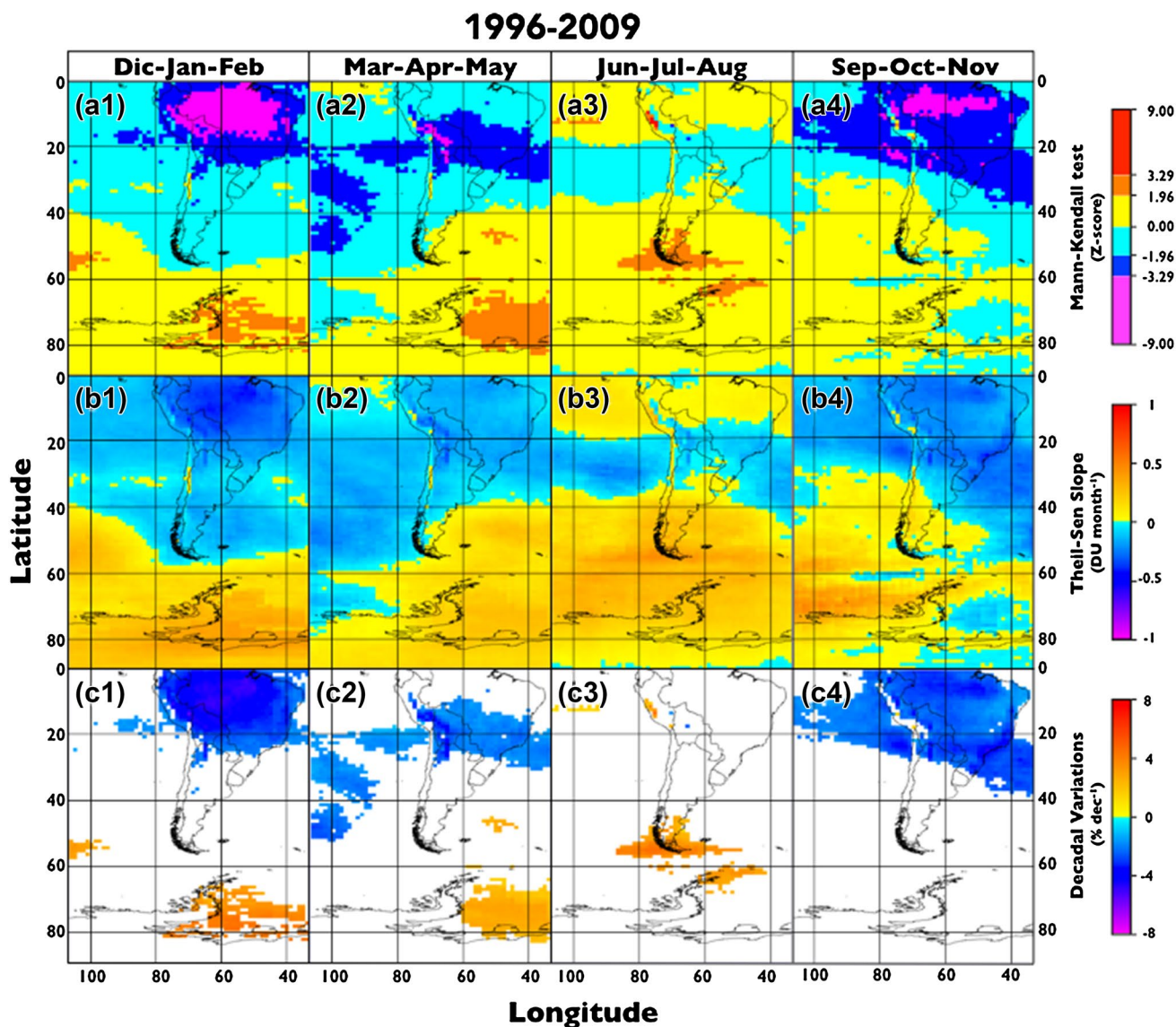
1996-2009

Fig. 6 Analysis of trends in the TOC from 1996 to 2009 for seasons defined as December, January and February (Dec–Jan–Feb), March, April and May (Mar–Apr–May), June, July and August (Jun–Jul– Aug) and September, October and November (Sep–Oct–Nov). Plots follow the same format as in Fig. 4

(-2.13% dec^{-1}) > Brasilia (-2.00% dec^{-1}) > Asunción (-1.62% dec^{-1}) > Salvador de Bahía (-1.17% dec^{-1}).

The pixel selected in the Antarctic region is the only location at which a statistically significant increase in TOC was observed from 1996 to 2009 (2.18% dec^{-1}). At a 95% confidence level, the increase was 0.17–4.34% dec^{-1}. These results suggest that although initial recovery of the TOC over the Antarctic began in 1996–2009, there were still decreases in the TOC over most of the middle to low latitude cities in South America.

3.6.1 Drivers of ozone levels

For the MLR, Fig. 7 shows the adjusted determination coefficients (adjusted-R^2, Fig. 7a), standardized partial correlation coefficients (partial-R, Fig. 7b) and magnitude of the fluctuations attributable to each proxy, represented by the magnitude of 2σ (Fig. 7c).

The adjusted-R^2 values generally range from 0.50 to 0.92 (red and brown colors in Fig. 7a), with some exceptions in the Andes Mountains and Patagonia (orange colors in Fig. 7a). These results indicate that on average,

Table 1 Summary of TOC trends in the most densely populated cities in the study area using the deseasonalized Theil-Sen method

City or place	Country	ID	Location °lat S, °long W, altitude (m)	1980–1995 Slope (% dec^{-1})	95% CI (% dec^{-1})	p	1996–2009 Slope (% dec^{-1})	95% CI (% dec^{-1})	p
Quito	Ecuador	QUI	00°15′ S, 78°35′ W, 2850	−1.56	−2.42 to −0.53	**	−1.14	−2.38 to 0.21	+
Guayaquil	Ecuador	GUA	02°11′ S, 79°53′ W, 4	−1.70	−2.58 to −0.79	***	−1.40	−2.64 to 0.02	+
Fortaleza	Brazil	FOR	03°43′ S, 38°32′ W, 21	−1.44	−2.10 to −0.74	***	−1.40	−2.45 to −0.26	*
Lima	Peru	LIM	12°02′ S, 77°01′W, 2672	−1.46	−1.97 to −0.85	***	−1.22	−2.06 to −0.38	*
Salvador de Bahía	Brazil	SAL	12°58′ S, 38°28′ W, 8	−1.86	−2.27 to −1.39	***	−1.17	−1.88 to −0.51	***
Brasilia	Brazil	BRA	15°48′ S, 47°52′ W, 1172	−1.46	−1.97 to −0.96	***	−2.00	−2.80 to −1.25	***
La Paz	Bolivia	LAP	16°30′ S, 68°09′ W, 3650	−0.15	−1.04 to 0.71	−	−2.13	−2.88 to −1.26	***
Belo Horizonte	Brazil	BEL	19°55′ S, 43°56′ W, 858	−2.05	−2.62 to −1.47	***	−2.40	−3.25 to −1.61	***
Río de Janeiro	Brazil	RIO	22°54′ S, 43°12′ W, 11	−2.35	−3.06 to −1.78	***	−2.15	−3.00 to −1.22	***
São Paulo	Brazil	SAO	23°33′ S, 46°38′ W, 760	−2.53	−3.24 to −1.92	***	−2.38	−3.30 to −1.43	***
Asunción	Paraguay	ASU	25°17′ S, 57°38′ W, 43	−2.19	−2.94 to −1.50	***	−1.62	−2.50 to −0.80	***
Santiago	Chile	SAN	33°27′ S, 70°40′ W, 567	−2.11	−2.86 to −1.33	***	0.48	−0.52 to 1.67	−
Buenos Aires	Argentina	BUE	34°36′ S, 58°22′ W, 25	−2.52	−3.34 to −1.69	***	−0.59	−1.68 to 0.46	−
Montevideo	Uruguay	MON	34°53′ S, 56°11′ W, 43	−2.45	−3.31 to −1.59	***	−0.65	−1.66 to 0.47	−
Punta Arenas	Chile	PUN	53°10′ S, 70°56′ W, 10	−5.09	−6.31 to −3.81	***	0.61	−1.14 to 2.49	−
Ushuaia	Argentina	USH	54°48′ S, 68°18′ W, 58	−5.44	−6.60 to −4.15	***	0.97	−0.77 to 2.95	−
Antarctica	Chile	ANT	73º00´ S, 62º30´ W, 780	−7.42	−9.29 to −5.49	***	2.18	0.17 to 4.34	*

The table shows the average slope in % dec^{-1} from 1980 to 2009 and 1996–2009. A 95% confidence interval for the slope and the p trend indicate statistically significant results; symbols next to each trend estimate indicate statistical significance, as follows: $p < 0.001 = ***$, $p < 0.01 = **$, $p < 0.05 = *$, $p < 0.1 = +$ and $p > 0.1 = -$ (no trend)

the model explains $73.9 \pm 8.1\%$ of the interannual variability in the TOC over the study area. At low latitudes, the model can explain more of the interannual TOC variability ($78.3 \pm 7.4\%$) than at high latitudes ($73.7 \pm 5.4\%$) and mid-latitudes ($69.5 \pm 8.5\%$). In other words, the model can better reproduce the low amplitudes of TOC variability observed at low latitudes but still performs well at high and mid-latitudes.

Based on the partial R (Fig. 7b) and 2σ (Fig. 7c) results, we suggest the following for each proxy:

YSC proxy Positive standardized partial correlation coefficients were observed over most of the study area. At low latitudes, the partial-R ranged from 0.7 to 0.9; the

partial-R value was smaller at middle (0.3–0.7) and high (0.0–0.5) latitudes (see Fig. 7, b1). This result can be explained by the fact that ozone formation is mediated by the intensity of UV radiation, which is directly correlated with the YSC. Given that the intensity of UV radiation decreases towards the poles, higher photochemical activity is observed at low latitudes. The MLR shows that the YSC's contribution to the variation in TOC is positive, reaching 3.0–7.0 DU at low latitudes and 1.0–5.0 DU over the remainder of the study area. These results indicate that the YSC is one of the driving factors that give rise to positive variations in the TOC at low and middle latitudes.
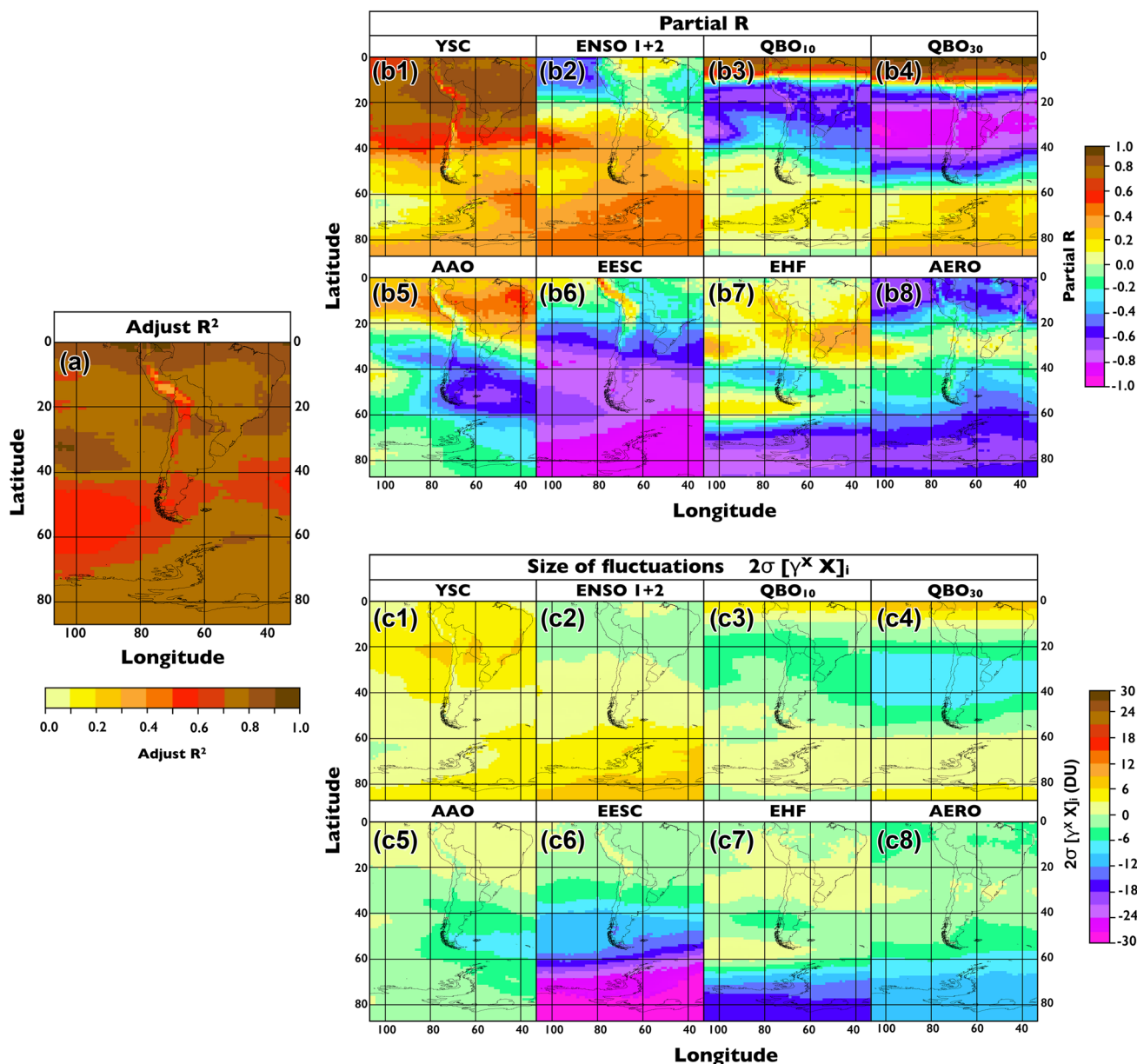
Fig. 7 MLR results, including the adjusted determination coefficients (adjusted-R^2, *left panel*), partial correlation coefficients (partial-R, *top panels* on *right*) and the size of fluctuations attributable to each proxy in the MLR, represented by the 2σ magnitude for each proxy (*bottom panels* on *right*)

$ENSO_{1+2}$ proxy Negative partial correlation coefficients were observed from 0°–20°S (partial-$R_{ENSO} < -0.7$), especially over the Pacific Ocean. Over the remainder of the study area, positive but lower partial correlation coefficients (<0.5) were observed (Fig. 7, b2). ENSO drives large-scale changes in ocean–atmosphere dynamics, affecting extratropical circulation. The warm ENSO phase is related to higher TOC values at middle to high latitudes (Newman et al. 2001; Randel et al. 2002; Bronnimann et al. 2004; Manzini et al. 2006; Chehade et al. 2014). The amount of TOC variability attributable to ENSO is negative at low

latitudes (−3.0 DU) and positive at middle (3.0 DU) and high (from 3.0 to 8.0 DU) latitudes (see Fig. 7, c2). Thus, the $ENSO_{1+2}$ proxy contributes moderately way to TOC variability at low and middle latitudes. However, this proxy has the greatest positive contribution to TOC variability at high latitudes (8.0 DU; see Fig. 7, b2, c2).

QBO proxy There are similar patterns in the partial-R coefficients for QBO at both 10 and 30 hPa. The positive regression estimates corresponding to the QBO index at the two pressure levels indicates a positive effect on TOC at lower latitudes (from 0° to 10° S, the partial-R ranges

from 0.50 to 0.87 for QBO_{10} and from 0.60 to 0.94 for QBO_{30}; see Fig. 7, b3, b4). At higher latitudes, the regression estimates switch to negative values (from 15° to 50°S, the partial-R ranges from −0.30 to −0.78 for QBO_{10} and from −0.30 to −0.93 for QBO_{30}; see Fig. 7, b3, b4). At high latitudes (above 50°S), there is a positive partial-R value (greater than 0.30; see Fig. 7, b4). This pattern could be related to a connection between the QBO and the BDC; Haklander et al. (2006) showed that the mean zonal wind pattern can alter wave driving of the BDC. The QBO_{10} contributes to ozone variability on the order of 3.0 to 6.0 DU between 0° and 10°S, from −2.0 to −4.0 DU between 15° and 50° S and from 1.0 to 3.0 DU between 50° and 90°S (see Fig. 7, c3). The QBO_{30} contributes to ozone variability on the order of 5.0–8.0, −2.0 to −9.0 and 2.0 to 5.0 DU, respectively, between 0° and 10°S, 15° and 50°S and 50° and 90°S (see Fig. 7, c4). These results indicate that QBO contributes moderately ozone variability at low and high latitudes and makes a greater contribution at mid-latitudes. QBO_{30} shows a greater contribution to interannual TOC variability than QBO_{10} in the study area.

AAO proxy The Antarctic Oscillation (AAO) is the dominant recurrent non-seasonal sea level pressure variation pattern south of 20° S and has been shown to contribute to ozone fluctuations (Fusco and Salby 1999; Hartmann et al. 2000; Appenzeller et al. 2000; Randel et al. 2002; Kiesewetter et al. 2010; Steinbrecht et al. 2003). Partial-R values smaller than 0.5 were observed over the entire study area. Two areas with higher partial-R values were observed at 10° S (greater than 0.6) and 50° S (lower than −0.6). It has been shown (Chehade et al. 2014) that the negative AAO phase enhances Southern Hemisphere ozone transport; however, the AAO contribution in the regression was only statistically significant for the zonal band from 45° to 55°S. Both the AAO and the QBO phase modulate wave propagation and are related to BDC variability (Baldwin et al. 2001). Our model shows that the AAO proxy contributes 2.0 to −2.0 DU to interannual TOC variations over the entire study area, except for the region at 50°S (covering most of Patagonia), where it drives TOC variations of −7.0 DU.

EESC proxy Partial-R values show that the EESC proxy has a negative effect on ozone outside of 20°S. The partial-R values increase with latitude (partial R < −0.6 beginning at 40°S), reaching values greater than 0.9 at high latitudes (>60°S). In contrast, lower partial-R values (0.2 to −0.4) were found in the tropical region (see Fig. 7, b6). The negative effects of the EESC proxy on ozone at mid- to high latitudes are consistent with the current understanding of EESC-driven ozone depletion (i.e., ozone chemistry). The size of the TOC variability attributed to the EESC proxy ranges from 1.0 to −3.0 DU, −6.0 to −20.0 DU and −20.0 to −30.0 DU, respectively, for low, middle and high

latitudes (see Fig. 7, c6). These results confirm that EESC is the main driver of interannual TOC variability over the study area.

EHF proxy Partial-R coefficients show positive values at latitudes below 60°S, with values less than 0.3. In contrast, the partial-R values reach 0.7 at high latitudes (over 60°S; see Fig. 7, b7). These results can be explained because the larger EHF values from 45° to 75°S (more negative values) indicate a stronger poleward flux of heat via eddies. This would give rise to higher TOC values at high latitudes as a result of a weaker Antarctic polar vortex. Therefore, the TOC variability attributed to the EHF proxy is maximized (reaching −17.0 DU) at higher latitudes. This contribution is only high above 70° S, but it is non-negligible at low latitudes, up to ±3.0 DU (see Fig. 7, c7).

AERO proxy Partial-R coefficients are negative over most of the study area. At low and high latitudes, the partial-R values reach −0.7 (see Fig. 7, b8). The long-term effects of stratospheric volcanic aerosols on global and polar ozone result from the increase in aerosol surface area density and subsequent heterogeneous ozone loss (Solomon 1999). Additionally, aerosols absorb infrared radiation, leading to a warmer lower stratosphere and thereby enhancing stratospheric dynamics and ozone depletion (e.g., Hadjinicolaou et al. 1997). The size of the TOC variability attributed to the AERO proxy at high latitudes is approximately −10.0 DU; at low and middle latitudes it is approximately −3 DU (see Fig. 7, c8). These results indicate that the AERO proxy has a lesser contribution to ozone variability at lower and middle latitudes and a moderate to high contribution at high latitudes. It has the third largest effect after the EESC and EHF contributions.

4 Atmospheric implications

The initial recovery of the Antarctic ozone layer can be observed from 1996 to 2009. A statistically significant increase in the TOC of 2% dec^{-1} was found at high latitudes (>60°S), showing the initial stage of TOC recovery over the Antarctic. However, the decreasing trend in the TOC continues over large areas of South America. Thus, it is necessary to continue the efforts that were made to protect the ozone layer through the Montreal Protocol, which has been the most successful multilateral environmental initiative in history.

The methodology used in this study allowed evaluation of the long-term trend in TOC over the study area and can be replicated in other studies. However, we note that the time series used in the analysis must be carefully chosen to result in statistically significant trends that appropriately describe monotonic variations. The time series must be chosen to avoid masking possible inflection points

without sacrificing the statistical robustness achieved by using a longer time series.

Statistically significant recovery of the TOC was observed for the months during which there is no polar vortex formation or other large-scale circulation processes that prevent redistribution of the ozone produced at the equator to extra-tropical areas. Despite evidence for the initial recovery of the TOC in some parts of the study area between 1996 and 2009, there is not yet a statistically significant long-term increase from September to November. In addition, large parts of the study area and most of the urban centers continue to show decreasing trends in the TOC. This indicates that the processes of destruction and depletion of stratospheric ozone resulting from the use of halogenated compounds continue, and remain more statistically significant than the initial signs of recovery identified in this article.

MLR analysis allowed us to identify and quantify the drivers governing interannual TOC variability in the study area. In our MLR model, the regression coefficients, adjusted R^2, standardized partial coefficients, and the magnitude of the fluctuations of the TOC can be attributed to each proxy for each pixel of the study area. This allows us to observe the space variability of the MLR model performance to explain the interannual fluctuations of the TOC in a part of the Southern Hemisphere.

The driving factors that led to greater interannual TOC variations at low latitudes were YSC, QBO_{10} and QBO_{30}, with a contribution on the order of 7 DU. At mid-latitudes, the most important drivers were $ENSO_{1+2}$, QBO_{30} and EESC, which contributed to the interannual variability on the order of 6 ($ENSO_{1+2}$) to -12 DU (EESC). Finally, at high latitudes, EESC is the most important determining factor for TOC variability, driving reductions of up to -30 DU, followed by EHF and AERO, which contributed approximately -17 and -11 DU, respectively. The effect of EHF, $ENSO_{1+2}$ and QBO_{30} at high latitudes is related to the intensity (strength) of the BDC, which transports heat and ozone from the equator where the ocean is warmer and equatorial zonal winds are more intense.

References

Albinana AP, Rubio J, Sanchez F, Vila M, Figuerola N, de Carcer IA, Jaque F (2000) Ozone transport in the mid-latitudes of South America in ozone hole conditions. P Soc Photo-Opt Ins 4131:315–322

Anton M, Lopez M, Serrano A, Banon M, Garcia JA (2010) Diurnal variability of total ozone column over Madrid (Spain). Atmos Environ 44(24):2793–2798

Anton M, Bortoli D, Costa MJ, Kulkarni PS, Domingues AF, Barriopedro D, Serrano A, Silva AM (2011a) Temporal and spatial variabilities of total ozone column over Portugal. Remote Sens Environ 115(3):855–863

Anton M, Bortoli D, Kulkarni PS, Costa MJ, Domingues AF, Loyola D, Silva AM, Alados-Arboledas L (2011b) Long-term trends of total ozone column over the Iberian Peninsula for the period 1979–2008. Atmos Environ 45(35):6283–6290

Antón M, Bortoli D, Kulkarni PS, Costa MJ, Domingues AF, Loyola D (2011) Long-term trends of total ozone column over the Iberian Peninsula for the period 1979–2008. Atmos Environ 45(35):6283–6290

Appenzeller C, Weiss AK, Staehelin J (2000) North Atlantic Oscillation modulates total ozone winter trends. Geophys Res Lett 27:1131–1134

Austin J, Struthers H, Scinocca J, Plummer D, Akiyoshi H, Baumgaertner JG (2010) Chemistry-climate model simulations of spring Antarctic ozone. J Geophys Res 5(115):D00M11

Baldwin M, Gray L, Dunkerton T, Hamilton K, Haynes P, Randel W, Holton J, Alexander M, Hirota I, Horinouchi T, Jones D, Kinnersley J, Marquardt C, Sato K, Takahashi M (2001) The Quasi-Biennial Oscillation. Rev Geophys 39:179–229

BAS (2012) Meteorology and Ozone Monitoring Unit—Antarctic ozone data, British Antarctic Survey [Internet]. Br Antarct Surv, Available from: http://www.antarctica.ac.uk/met/jds/ozone/index.html

Bates DR, Nicolet M (1950) The photochemistry of atmospheric water vapor. J Geophys Res 55(3):301–327

Bodeker GE, Shiona H, Eskes H (2005) Physics Indicators of Antarctic ozone depletion. Atmos Chem Phys 5:2603–2615

Brewer AW (1949) Evidence for a world circulation provided by the measurements of helium and water vapour distribution in the stratosphere. Q J R Meteorol Soc 75(326):351–363

Bronnimann S, Luterbacher J, Staehelin J, Svendby T, Hansen G, Svenoe T (2004) Extreme climate of the global troposphere and stratosphere in 1940–42 related to El Niño. Nature 431:971–974

Carslaw D, Ropkins K (2012) Openair an R package for air quality data analysis. Environ Mod Soft 27–28:52–61

Casiccia C, Zamorano F (2008) Erythemal irradiance at the Magellan's region and Antarctic ozone hole 1999–2005. Atmósfera 21(1):1–12

Casiccia C, Kirchhoff VWJH, Torres A (2003) Simultaneous measurements of ozone and ultraviolet radiation: spring 2000, Punta Arenas, Chile. Atmos Environ 37(68):383–389

Chapman S (1930) On ozone and atomic oxygen in the upper atmosphere. Dublin Philos Mag J Sci 10(64):369–83

Chehade W, Weber M, Burrows JP (2014) Total ozone trends and variability during 1979–2012 from merged data sets of various satellites. Atmos Chem Phys 14:7059–7074

Cionni I, Eyring V, Lamarque JF, Randel WJ, Stevenson DS, Wu F (2011) Ozone database in support of CMIP5 simulations: results and corresponding radiative forcing. Atmos Chem Phys 11(21):11267–11292

de Artigas MZ, de Campra PF (2010) Trends in total ozone and the effect of the equatorial zonal wind QBO. J Atmos Sol-Terr Phy 72(7–8):565–569

de Laat ATJ, van der ARJ, Allaart MAF, van Weele M, Benitez GC, Casiccia C (2010) Extreme sunbathing: Three weeks of small total O3 columns and high UV radiation over the southern tip of South America during the 2009 Antarctic O$_3$ hole season. Geophys Res Lett 37(14):L14805

Dobson GMB (1956) Origin and distribution of the polyatomic molecules in the atmosphere. Proc R Soc A Math Phys Eng Sci 236(1205):187–93

Durbin J, Watson GS (1950) Testing for serial correlation in least squares regression. I. Biometrika 37:409–428

Fogg GE (2000) The Royal Society and the Antarctic. Notes Rec R Soc 54(1):85–98

Frossard L, Rieder HE, Ribatet M, Staehelin J, Maeder JA, Di Rocco S, Davison AC, Peter T (2013) On the relationship between total ozone and atmospheric dynamics and chemistry at midlatitudes—Part 1: Statistical models and spatial fingerprints of atmospheric dynamics and chemistry. Atmos Chem Phys 13:147–164

Fusco AC, Salby ML (1999) Interannual Variations of Total Ozone and Their Relationship to Variations of Planetary Wave Activity. J Climate 12:1619–1629

Geller MA, Smyshlyaev SP (2002) A model study of total ozone evolution 1979–2000—the role of individual natural and anthropogenic effects. Geophys Res Lett 29(22)

Godin-Beekmann S (2010) Spatial observation of the ozone layer. Comptes Rendus Geosci Academie des Sciences 342(4–5):339–348

Hadjinicolaou P, Pyle JA, Chipperfield MP, Kettleborough JA (1997) Effect of interannual meteorological variability on mid-latitude O3. Geophys Res Lett 24:2993–2996

Haklander AJ, Siegmund PC, Kelder HM (2006) Analysis of the frequency-dependent response to wave forcing in the extratropics. Atmos Chem Phys 6:4477–4481

Harris JM, Oltmans SJ, Bodeker GE, Stolarski R, Evans RD, Quincy DM (2003) Long-term variations in total ozone derived from Dobson and satellite data. Atmos Environ 37(23):3167–3175

Harris NRP, Kyrö E, Staehelin J, Brunner D, Andersen S-B, Godin-Beekmann S (2008) Ozone trends at northern mid- and high latitudes – a European perspective. Ann Geophys 26(23):1207–1220

Hartmann DL, M Wallace J, Limpasuvan V, Thompson D, Holton JR (2000) Can ozone depletion and global warming interact to produce rapid climate change? P Natl Acad Sci USA 97:1412–1417

Hassler B, Bodeker GE, Solomon S, Young PJ (2011) Changes in the polar vortex: effects on Antarctic total ozone observations at various stations. Geophys Res Lett 38

Horel J, Wallace J (1981) Planetary-scale atmospheric phenomena associated with the southern oscillation. Am Meteor Soc 109:813–829

Iqbal M (1983) An introduction to solar radiation. An Introd Sol Radiat. Elsevier pp 59–84

Jain SL, Kulkarni PS, Ghude SD, Polade SD, Arya BC, Dubey PK (2008) Trend analysis of total column ozone over New Delhi, India. Mapan-J Metrol Soc I 23(2):63–69

Jiang X, Pawson S, Camp CD, Nielsen JE, Shia R-L, Liao T, Limpasuvan V, Yung YL (2008a) Interannual variability and trends of extratropical ozone. Part I: Northern Hemisphere. J Atmos Sci 65(10):3013–3029

Jiang X, Pawson S, Camp CD, Nielsen JE, Shia R-L, Liao T, Limpasuvan V, Yung YL (2008b) Interannual Variability and Trends of Extratropical Ozone. Part II: Southern Hemisphere. J Atmos Sci 65(10):3030–3041

Kane RP (1998b) Ozone depletion, related UVB changes and increased skin cancer incidence. Int J Climatol 18:457–472

Kane RP, Sahai Y, Casiccia C (1998a) Latitude dependence of the quasi-biennial oscillation and quasi-triennial oscillation characteristics of total ozone measured by TOMS. J Geophys Res-Atmos 103(D7):8477–8490

Kaniaru D (2007) The montreal protocol: celebrating 20 Years of environmental progress: ozone layer and climate protection. UNEP/Earthprint, p 355

Kanitz T, Seifert P, Ansmann A, Engelmann R, Althausen D, Casiccia C (2011) Contrasting the impact of aerosols at northern and southern midlatitudes on heterogeneous ice formation. Geophys Res Lett 38(17):L17802

Karoly D (1989) Southern hemisphere circulation features associated with El Niño-Southern oscillation events. Am Meteor Soc 12:1239–1252

Kiesewetter G, Sinnhuber BM, Weber M, Burrows JP (2010) Attribution of stratospheric ozone trends to chemistry and transport: a modelling study. Atmos Chem Phys 10:12073–12089

Kirchhoff VWJH, Casiccia CARS, Zamorano BF (1997) The ozone hole over Punta Arenas, Chile. J Geophys Res 102(D7):8945–8953. doi:10.1029/96JD03609

Krueger AJ, Guenther B, Fleig AJ, Heath DF, Hilsenrath E, McPeters R (1980) Satellite ozone measurements. Philos Trans R Soc A Math Phys Eng Sci 296(1418):191–204

Labitzke K, VanLoon H (1997) The signal of the 11-year sunspot cycle in the upper troposphere lower stratosphere. Space Sci Rev 80(3–4):393–410

Lee H, Smith AK (2003) Simulation of the combined effects of solar cycle, quasi-biennial oscillation, and volcanic forcing on stratospheric ozone changes in recent decades. J Geophys Res-Atmos 108(D2)

Lindfors A, Vuilleumier L (2005) Erythemal UV at Davos (Switzerland), 1926–2003, estimated using total ozone, sunshine duration, and snow depth. J Geophys Res 110(D2):D02104

Malanca FE (2005) Trends evolution of ozone between 1980 and 2000 at midlatitudes over the Southern Hemisphere: Decadal differences in trends. J Geophys Res 110(D5):D05102

Manzini E, Giorgetta MA, Esch M, Kornblueh L, Roeckner E (2006) The influence of sea surface temperatures on the northern winter stratosphere: ensemble simulations with the MAECHAM5 model. J Climate 19:3863–3881

McCormack JP, Siskind DE, Hood LL (2007) Solar-QBO interaction and its impact on stratospheric ozone in a zonally averaged photochemical transport model of the middle atmosphere. J Geophys Res 112(D16109)

Molina MJ, Rowland FS (1974) Stratospheric sink for chlorofluoromethanes: chlorine atom catalysed destruction of ozone. Nature 249(5460):810–812

Monreal McMahon R, Aguilar R, Valderrama V, Burt PJA (2002) An operational method for forecasting total column ozone for Punta Arenas, Chile. Meteorol Appl 9(3):327–333

Müller R, Grooß J, Lemmen C, Heinze D, Dameris M, Bodeker G (2008) Simple measures of ozone depletion in the polar stratosphere. Atmos Chem Phys 8:251–264

Munir S, Chen H, Ropkins K (2013) Quantifying temporal trends in ground level ozone concentration in the UK. Sci Total Environ 458–460:217–227

NASA (2012) Ozone Hole Watch, National Aeronautics and Space Administration, Goddard Space Flight Center [Internet]. [cited 2014 Nov 6]. Available from: http://ozonewatch.gsfc.nasa.gov/

Newman PA, Nash ER, Rosenfield JE (2001) What controls the temperature of the Arctic stratosphere during the spring? J Geophys Res 106(D17):19999–20010. doi:10.1029/2000JD000061

Nicolet M (1955) The aeronomic problem of nitrogen oxides. J Atmos Terr Phys 7:152–169

Ningombam SS (2011) Variability of sunspot cycle QBO and total ozone over high altitude western Himalayan regions. J Atmos Sol-Terr Phy 73(16):2305–2313

Niu X, Frederick JE, Stein ML, Tiao GC (1992) Trends in column ozone based on TOMS data: dependence on month, latitude, and longitude. J Geophys Res 97(D13):14661–14669. doi:10.1029/92JD01392

Perez-Albinana A, Rubio J, Sanchez J, Vila M, Figuerola N, Aguirre de Carcer I (2000) Ozone transport in the mid-latitudes of South America in ozone hole conditions. International Society for Optics and Photonics pp 315–322

Randel WJ, Wu F, Stolarski R (2002) Changes in column ozone correlated with the stratospheric EP flux. J Meteorol Soc Jpn 80:849–862

Rieder HE, Staehelin J, Maeder J, Peter T, Ribatet M, Davison C (2010a) Extreme events in total ozone over Arosa – Part 1: Application of extreme value theory. Atmos Chem Phys 10(20):10021–10031

Rieder HE, Staehelin J, Maeder J, Peter T, Ribatet M, Davison C (2010b) Extreme events in total ozone over Arosa—Part 2: Fingerprints of atmospheric dynamics and chemistry and effects on mean values and long-term changes. Atmos Chem Phys 10(20):10033–10045

Sato M, Hansen JE, McCormick MP, Pollack JB (1993) Stratospheric aerosol optical depths, 1850–1990. J Geophys Res-Atmos 98:22987–22994

Shindell D, Rind D, Balachandran N, Lean J, Lonergan P (1999) Solar cycle variability, ozone, and climate. Science 284:305–308

Shiotani M (1992) Annual, Quasi-Biennial, and E1 Niño-Southern Oscillation (ENSO) Time-Scale Variations in Equatorial Total Ozone. J Geophys Res 97(D7):7625–7633

Sola Y, Lorente J (2010) Impact of two low ozone events on surface solar UV radiation over the northeast of Spain. Int J Climatol 31:1724–1734

Solomon S (1999) Stratospheric ozone depletion: a review of concepts and history. Rev Geophys 37:275–316

SPARC (2006) SPARC Assessment of Stratospheric Aerosol Properties (ASAP). Thomason L and Peter T Eds. SPARC Report No. 4, WCRP-124, WMO/TD—No. 1295

Staehelin J, Thudium J, Buehler R, Volz-Thomas A, Graber W (1994) Trends in surface ozone concentrations at Arosa (Switzerland). Atmos Environ 28(1):75–87

Staehelin J, Renaud A, Mcpeters R, Viatte P, Hoegger B, Bugnion V (1998) Total ozone series at Arosa (Switzerland): Homogenization and data comparison. J Geophys Res 103(D5):5827–5841. doi:10.1029/97JD02402

Staehelin J, Harris NRP, Appenzeller C, Eberhard J (2001) Ozone trends: a review. Rev Geophys 39(2):231–290

Staehelin J, Vogler C, Br S (2009) The long history of ozone measurements: climatological information derived from long ozone records. Zerefos, Christos, Contopoulos, G., Skalkeas G Springer; 2009. Pp 119–131

Steinbrecht W, Hassler B, Claude H, Winkler P, Stolarski RS (2003) Global distribution of total ozone and lower stratospheric temperature variations. Atmos Chem Phys 3:1421–1438

Struthers H, Bodeker GE, Austin J, Bekki S, Cionni I, Dameris M (2009) The simulation of the Antarctic ozone hole by chemistry-climate models. Atmos Chem Phys 9:6363–6376

Tandon A, Attri AK (2011) Trends in total ozone column over India: 1979–2008. Atmos Environ 45(9):1648–1654

Toro R, Morales RGE, Canales M, Gonzales C, Leiva M (2014) Inhaled and inspired particulates in metropolitan Santiago Chile exceed air quality standards. Build Environ 79:115–123

UNEP (2003) Handbook for the International Treaties for the Protection of the Ozone Layer. 6th edn. The secretariat for The Vienna convention for the protection of the ozone layer and the montreal protocol on substances that deplete the ozone layer, United Nations Environment Programme

Weatherhead EC, Reinsel GC, Tiao GC, Jackman CH, Bishop L, Hollandsworth SM (2000) Detecting the recovery of total column ozone. J Geophys Res 105(17):201–210

Weber M, Dikty S, Burrows JP, Garny H, Dameris M, Kubin A, Abalichin J, Langematz U (2011) The Brewer–Dobson circulation and total ozone from seasonal to decadal time scales. Atmos Chem Phys 11:11221–11235

Werner R (2008) The latitudinal ozone variability study using wavelet analysis. J Atmos Solar-Terrestrial Phys 70(2–4):261–267

Witte JC, Schoeberl MR, Douglass AR, Thompson AM (2008) The Quasi-biennial Oscillation and annual variations in tropical ozone from SHADOZ and HALOE. Atmos Chem Phys 8:3929–3936

WMO (2010) World Meteorological Organization. Scientific assessment of ozone depletion: Global ozone research and monitoring project. Technical Report 52, Geneva, Switzerland

WMO (2014) World Meteorological Organization. Scientific assessment of ozone depletion: 2014. Global Ozone Research and Monitoring Project. Report No. 55, Geneva, Switzerland

Ziemke JR, Chandra S (2003) La Nina and El Nino-induced variabilities of ozone in the tropical lower atmosphere during 1970–2001. Geophys Res Lett 30(3)

Ziemke JR, Chandra S, Oman LD, Bhartia PK (2010) A new ENSO index derived from satellite measurements of column ozone. Atmos Chem Phys 10(8):3711–3721